# Optimized solar cells based on changes in resonance structure as a function of the refractive index and the thickness

Maren Anna Brandsrud[a], Rozalia Lukacs[a], Reinhold Blümel[b], Eivind Seim[a], Erik Stensrud Marstein[c,d], Espen Olsen[a], and Achim Kohler[a]

[a]Norwegian University of Life Sciences, Faculty of Science and Technology, Drøbakveien 31, 1432 Ås, Norway
[b]Wesleyan University, Department of Physics, 265 Church Street, Middletown, CT 06459, United States of America
[c]Institute of Energy, Department of Solar Energy, Instituttveien 18, 2007 Kjeller, Norway
[d]University of Oslo, Department of Technology Systems, Gunnar Randers Vei 19, 2007 Kjeller, Norway

## ABSTRACT

In order to reduce costs, the solar cell industry is aiming at producing ever thinner solar cells. Structuring the surfaces of optically thin solar cells is important for avoiding excessive transmission-related losses and, hence, to maintain or increase their efficiency. Light trapping leading to longer optical path lengths within the solar cells is a well established field of research. In addition to this, other possible benefits of structured surfaces have been proposed. It has been suggested that nanostructures on the surface of thin solar cells function as resonators, inducing electric-field resonances that enhance absorption in the the energy-converting material. Further, coupling of electric field resonances in periodically structured solar cells may couple with each other thereby increasing the absorption of energy. A deeper understanding of the nature of the energy-conversion enhancement in surface-structured and thin solar cells would allow to design more targeted structures.

Generally, efficiency enhancement may be evaluated by investigating the electric field and optimizing the optical generation rate. Here, we establish a model system consisting of multilayered solar cells in order to study resonances and coupling of resonances in a one-dimensional system. We show that resonances in energy-converting and non-energy converting layers exist. The coupling of resonances in the non-energy converting material and the energy-converting material is only possible for certain parameter ranges of thickness of the energy converting material and the imaginary part of the refractive index. We evaluate the resonances and the coupling of resonances in different thin-film systems and show how they affect the total absorption of energy in the energy converting layer. We show how resonances in non-absorbing layers can contribute to increasing the resonances in the absorbing layers. We optimize the parameters of the multilayered thin-film systems to achieve an increase in the amount of the absorbed energy. The optimization is also evaluated for an experimentally realizable thin-film solar cell.

**Keywords:** Optimization, optically thin solar cells, absorption cross section, resonances

## 1. INTRODUCTION

The solar-cell industry is continuously on the lookout for ways to reduce material usage in the production of solar cells while maintaining conversion efficiency in order to increase the cost-efficiency of solar-cell devices.[1,2] While thin, crystalline silicon solar cells exhibit lower absorption than thicker, traditionally crystalline silicon wafer cells,[1] absorption in optically thin solar cells can be enhanced by surface structuring, e.g., by adding surface structures to the top layer of thin solar cells.[3,4] The most established approach is light trapping, wherein the path length of light in the absorber is increased because of the surface structures. It has also been shown

Further author information: (Send correspondence to M.A.B.)
M.A.B.: E-mail: maren.brandsrud@nmbu.no

that resonances of the electric field due to the structured surface increases the absorption in the absorptive material below.[3] Coupling of resonances in the structures can also yield absorption enhancement in structured thin film solar cells.[5] Another way to enhance efficiency of thin solar cells is to minimize the energy losses due to reflection.[6] A possible way to achieve this is to add one or more thin dielectric layers on the top of the solar cell as anti-reflection coatings (ARC). Single layer ARCs are standard in the industry today. However, many works have carried out optimization of the different layers to find the optimum combination of the refractive indexes (materials) and thicknesses.[7]

The aim of the current study was to study absorption efficiency in the energy converting layer of a solar cell as a function of resonances in the absorbing and non-absorbing layers of a thin-film solar cell. To this purpose we want to develop a simple model system that exhibits resonances and allows to investigate the implication of these resonances on absorption in the energy converting material. A simple system that can exhibit resonances is a multilayered-film system. A multilayered film system can be set up by absorbing and non-absorbing layers. It can be used to investigate how resonances in the non-absorbing layers affect the absorption in the absorbing layers. It can be further used to investigate, how absorption can be enhanced by tuning the refractive index and the thicknesses of the absorbing and non-absorbing layers involved. Therefore our work is strongly related to optimization of anti-reflection coatings,[6] but it focuses on a different aspect, namely the effect of resonances in layered films on the absorption in the energy converting film.

In order to study the effectiveness of the device, we evaluate the absorption cross section, $\sigma_a$.[8,9] The absorption cross section is similar to the optical generation rate,[10] while the optical generation rate is taking into account a weighting by the solar spectrum. The system that is evaluated in our work is a one dimensional system where the incoming light is propagating towards the system where the propagation direction is perpendicular to the surface. This system is equivalent to an three dimensional system with normal incident light.

The paper is organized as follows: In Sec. 2, systems with wavelength independent refractive indices are evaluated. We investigate how the absorption cross section and the resonant structure in the layered film depend on the size of the imaginary part of the refractive index. We show that our results agree with the Fresnel equations[11] for non-magnetic dielectric materials. We investigate further if the thickness of the layers can be optimized with respect to absorption efficiency and material usage. We show how a resonance in the non-absorptive material enhances the absorption of light in the energy converting film. Sec. 2 also illustrates that optimization of film thickness is more beneficial for systems with a larger range for the refractive indices. We further demonstrate that our approach can be useful in the optimization of real solar cell material by optimizing the thickness of the layers of an experimentally realizable solar cell in Sec. 3.

## 2. OPTIMIZATION OF ABSORPTION CROSS SECTION FOR THIN-FILM SYSTEMS WITH CONSTANT REFRACTIVE INDEX

Optically thin solar cells with normal incidence can be treated as one-dimensional systems and are therefore simple to handle numerically. The model system chosen in the current paper represents a one-dimensional system consisting of several thin layers with different absorbing and non-absorbing materials. Both the non-absorbing and the absorbing materials can function as resonators as we will see later. In the first part of the paper, we consider thin-film systems with an index of refraction that is independent of the wavelength as shown in Fig. 1. We assume that the backside of the film is a perfect mirror, reflecting back all the radiation perfectly. We assume further that the incoming light is a plane wave with an amplitude equal to 1. Since we only consider normal incidence and thus treat the model system in one dimension, we do not need to consider the polarization. Thus, the model system can be described by scalar wave theory, which provides an exact description of the wave mechanics in the film structures.The one dimensional model is completely equivalent to to the three dimensional film system with normal incident light.

For the layered systems shown in Fig. 1, generally the amount of absorbed light can be calculated via the absorption cross section $\sigma_a$ given by

$$\sigma_a = 1 - |r|^2, \tag{1}$$

where $r$ is the amplitude of the reflected plane wave,[8,9] while $|r|^2 = R$ is the reflection probability of the system. When the refractive index is real for all films involved, $|r|^2 = 1$ and the absorption cross section $\sigma_a = 0$.

The amplitude of the reflected wave can be found by requiring a continuous scalar wave function and a continuous first derivative of the scalar wave function at all interfaces.[12,13] For simple systems with a few layers of materials, as the ones presented in Fig. 1, the calculation of $\sigma_a$ is straightforward. For systems consisting of several layers, the transfer matrix method[14] may be used. Alternatively, a hierarchical summation scheme suggested by Brandsrud et. al.[8] can be employed.


(a) (b)

Figure 1: A thin-film system consisting of (a) two and (b) three films. The film system starts at $x = 0$. Outside the film we assume vacuum with a refractive index of $n_0 = 1$. The boundaries between the films are at $x = a$ and $x = b$. At $x = m$ a perfect mirror is placed. The refractive indices of the thin-film layers $I$, $II$ and $III$ are given by $n_I$, $n_{II}$ and $n_{III}$, respectively. The film closest to the mirror represents the energy-converting material, i.e. the index of refraction is complex. The light is propagating from left with an normal incidence.

## 2.1 Two-film system

We will now demonstrate how the absorption efficiency of a two-layered system, as shown in Fig. 1a, depends on the resonance structure in the absorbing and non-absorbing films. This knowledge can be used to optimize the absorption efficiency as a function of the refractive indices of the films and the thicknesses of the two layers. The absorption efficiency can be either optimized (i) for a certain wavelength, (ii) for a wavelength region, or (iii) for the entire solar spectrum.

### 2.1.1 The importance of the size of the imaginary part of the refractive index of the absorptive material

We start with investigating how the absorption efficiency depends on the imaginary part of the refractive index of the absorptive film. For the study, we consider the two-film system shown in Fig. 1a. We set the refractive index of the first film to 1.5. Thus, the first film is the non-absorbing material. The second film is the absorbing material with a complex refractive index. We set the real part of the refractive index of the second film to 1.8. The imaginary part of the refractive index of the second film, $\Im(n_{II})$, determines the absorption properties of the material. The imaginary part of the refractive index of the second film, $\Im(n_{II})$, is our tuning parameter and is varied from $\Im(n_{II}) = 0.1$ to $\Im(n_{II}) = 0.8$. The thicknesses of the first and second film are chosen to be 216 nm and 500 nm, respectively. We will now study the absorption cross section $\sigma_a$ as a function of imaginary part of the refractive index of the second film $\Im(n_{II})$.

Figure 2a shows the absorption cross section $\sigma_a$ as a function of wavelength for different values of the imaginary part of the refractive index, $\Im(n_{II})$, of the second film. For example for $\Im(n_{II}) = 0.1$, a clear resonant structure can be observed in $\sigma_a$. A resonance, i.e. a peak, in the absorption cross section $\sigma_a$ means that the absorption of the light is enhanced for certain wavelengths compared with the neighboring wavelengths. We see that the resonance structure of the absorption cross section $\sigma_a$ strongly depends on the size of the imaginary part of the refractive index in the second film $\Im(n_{II})$: For the smallest $\Im(n_{II})$, the resonance structure of the absorption shows rapid oscillations. When we increase $\Im(n_{II})$, slower oscillation of the resonance structure can be observed. Figure 2b shows the average absorption cross section, $\bar{\sigma_a}$, as a function of $\Im(n_{II})$. The average absorption cross section $\bar{\sigma_a}$ is calculated as the mean of wavelength range 200-1200 nm. We may also investigate $\bar{\sigma_a}$ for other wavelength regions. When we increase $\Im(n_{II})$, $\bar{\sigma_a}$ increases slowly until the value $\Im(n_{II}) = 0.32$ is reached. After this $\bar{\sigma_a}$ decreases as $\Im(n_{II})$ increases further. This agrees with Fresnel's equations.[11]

The resonance structure of the absorption cross section $\sigma_a$ shown in Fig. 2a can be interpreted physically as follows: For small $\Im(n_{II})$, the incident electromagnetic wave creates standing waves in both films. The standing

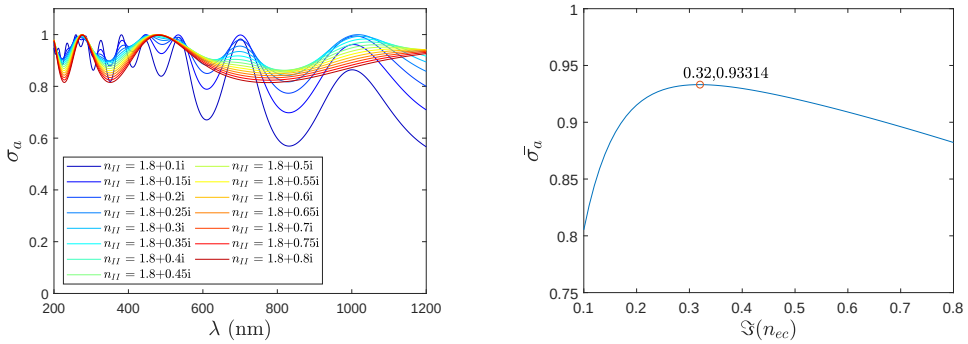


(a) (b)

Figure 2: A constant real part of the refractive indices for both of the films, $n_I = 1.5$ and $\Re(n_{II}) = 1.8$ is assumed. The imaginary part of the second film $\Im(n_{II})$ is varied between 0.1 and 0.8. The thicknesses of the films were kept constant at 216 nm for the first film and at 500 nm for the second film. (a) shows $\sigma_a$ as a function of wavelength (200 nm - 1200 nm) for all considered $\Im(n_{II})$ values and (b) shows the average of $\sigma_a$ for the whole wavelength range as function of $\Im(n_{II})$. The optimal value of $\Im(n_{II})$ is 0.32 and gives an $\bar{\sigma_a} = 0.933288$. This point is marked with the red circle on (b).

waves produce an increased electromagnetic field inside the films, which results in an increase of the absorption of light. As we increase $\Im(n_{II})$ more radiation is absorbed in the second film, and at one point all radiation that enters the second film is absorbed before it reaches the mirror. From this point the resonance structure depends only on the resonances in the first film. This is illustrated in Fig. 3a and Fig. 3b, where different standing waves inside the first or the first and the second film are shown for $\Im(n_{II}) = 0.3$ and $\Im(n_{II}) = 0.8$, respectively. The absolute square of the scalar wave function, $|\psi|^2$, is plotted for all wavelengths that correspond to the resonances shown in Fig. 2a. In Fig. 3a we see that for $\Im(n_{II}) = 0.3$ the small wavelengths are totally absorbed before they reach the mirror and the long wavelengths still create a standing wave in the second film, while in Fig. 3b standing waves have only resonances in the first film and are totally absorbed in the second film.

Inspecting Fig. 2b, we find that the best choice of $\Im(n_{II})$ is 0.32. This optimum is in the transition zone between the two types of resonance structures, that can be seen in Fig. 2a: the one with the higher oscillations and the one with the smaller oscillations.

### 2.1.2 The importance of the thickness of the absorptive material

It is obvious from the discussion in the previous section that for a given standing wave that extends over both films such as the standing waves at the wavelengths 697 nm and 1025 nm in Fig. 3a, an increase of the film thickness would lead to a further increase of $\sigma_a$, since with increasing film thickness, an increasing amount of the radiation is absorbed in the second film and the resonant structure in the second film will gradually disappear. However, since an increase in thickness means an increase in material costs, it is important to determine the optimal thickness. In fact, an increase of the thickness of the absorptive film, i.e. the second film in in Fig. 1a, changes the resonance structure more drastically than an increase of the imaginary part.

Figure 4a shows how $\sigma_a$ changes with increasing thickness of the absorptive film. Eventually, when an optimal thickness is achieved, the average $\sigma_a$ does not increase further. For larger thicknesses, the plane wave that enters the absorptive film is totally absorbed before it reaches the mirror and a further increase in thickness does not increase absorption efficiency further.

Figure 5 shows the absolute square of the wave function, $|\psi|^2$, for a two-film system with a wavelength-independent refractive index for two film thicknesses of the second film: In (a) a thickness of 871 nm and in (b) a thickness of 1500 nm is used for the second film. The absolute square of the wave function, $|\psi|^2$, is plotted for the resonances indicated in Fig. 4a. Figure 5a shows that for small wavelengths, $|\psi|^2$ is completely absorbed before it reaches the mirror. For the longer wavelengths, $|\psi|^2$ is not completely absorbed in the second film. The incoming radiation reaches the mirror and forms a standing wave that extends over both films.

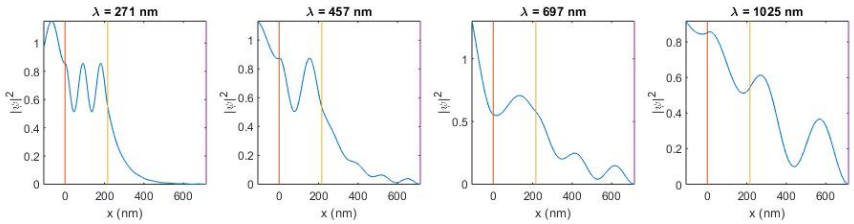


(a)

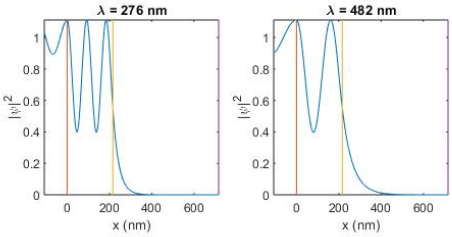


(b)

Figure 3: The absolute square, $|\psi|^2$, of the scalar wave function is shown for wavelengths corresponding to the resonant wavelengths shown in Fig. 2a. The red line indicates the boundary between vacuum and first layer, the yellow line indicates the boundary between the two films, and the purple line indicates the mirror. For both films the refractive indices are constant. For the first film the refractive index is real with the value $n_I = 1.5$. The refractive index of the second film is $n_{II} = 1.8 + 0.3i$ in (a) and $n_{II} = 1.8 + 0.8i$ in (b). The thicknesses of the films are kept constant at 216 nm for the first film and at 500 nm for the second film. The wave structure of $|\psi|^2$ in front of the first layer is due to the superposition of the incident and reflected wave.

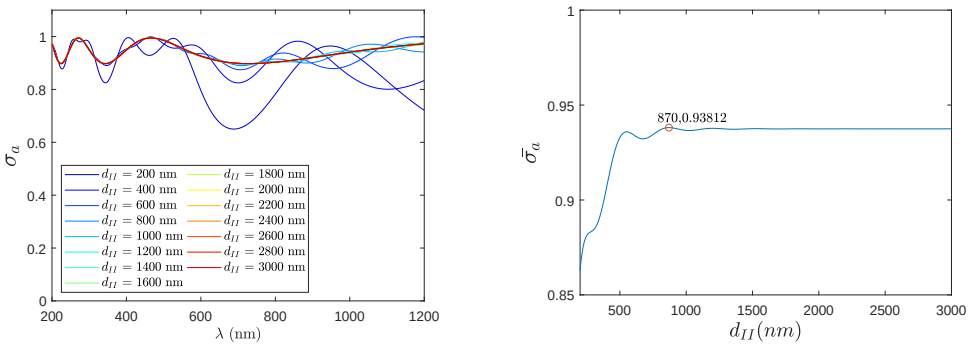


(a) (b)

Figure 4: The absorption cross section $\sigma_a$ is shown as a function of wavelength for the spectral range 200 nm to 1200 nm in (a). In (b) the average of $\sigma_a$ for the same wavelength, is shown range as a function of the thickness of the second film, $d_{II}$. The refractive indices are constant for both films, with $n_I = 1.5$ and $n_{II} = 1.8 + 0.3i$. The thickness of the first film is kept constant at 216 nm. $d_{II}$ changes between 200 nm and 3000 nm. We find that the optimal thickness of the second film is 871 nm, yielding a maximum absorption cross section of $\bar{\sigma_a} = 0.93812$ as marked with a red circle in figure (b).

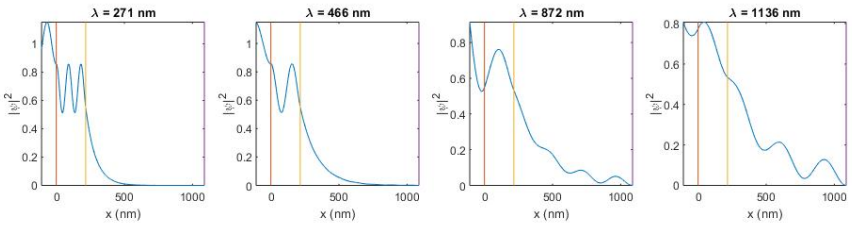


(a)

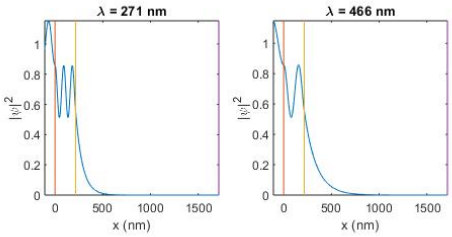


(b)

Figure 5: The absolute square of the scalar wave function $|\psi|^2$ is shown for wavelengths that correspond to the resonances shown in Fig. 4a. The red line indicates the boundary between vacuum and first film, the yellow line indicates the boundary between the two films, and the purple line indicates the mirror. The refractive indices are constant for both films and are given by $n_I = 1.5$ and $n_{II} = 1.8 + 0.3i$, respectively. The thickness of the first film is kept constant at 216 nm; the thickness of the second film is set to 871 nm in (a) and 1500 nm in (b). The wave structure in front of the first layer is due to the superposition of the incident and reflected wave.

In Fig. 5b the absolute square of the wave function, $|\psi|^2$, is plotted for the wavelengths in Fig. 4a that show resonances for the case of an increased film thickness. We observe that the radiation is completely absorbed before the mirror is reached. Therefore, we can conclude that in this case, maxima in the absorption cross section $\sigma_a$ depend only on standing waves in the first non-absorbing film. This is an important finding: in our model system, absorption increases solely due to resonant structures. This effect is not mixed with other effects that could be considered as possible explanations for absorption enhancement, such as coupling of resonances[15] and ray trapping.[16–18] When the condition for standing waves is satisfied in the first film, $|\psi|^2$ increases. Since $|\psi|^2$ is continuous across the boundary between the two films, it follows that $|\psi|^2$ also increases inside the absorptive film. Hence, the absorption in the film increases and the reflection probability decreases.

## 2.2 Optimization of three-film system

In order to approach more complex thin-film systems, a three-layered film system with a mirror, as in Fig. 1b, is evaluated. As for the two-film systems, the refractive indices of the films are constant for all wavelengths. This is to highlight the effect of the thickness of the first two layers on the average of the absorption cross section, $\bar{\sigma_a}$. The thickness of the third, absorptive film is chosen such that the wave function in this film is totally absorbed.

In Fig. 6a shows a three film system, where the refractive indices of layer I, II and III in Fig. 1b are set to 1.5, 1.65 and $1.8 + 0.03i$, respectively. The thickness of the third layer is set to 1000 nm. The thickness of the two first layers in the system are varied between 20 nm and 1000 nm in order to optimize the thicknesses of the two films with respect to the absorption efficiency of the third film. Figure 6a shows the average absorption cross section, $\bar{\sigma_a}$, for different combinations of the thicknesses of two first layers. We consider the wavelength range from 200 nm to 1200 nm. In Fig. 6b, $\bar{\sigma_a}$ for a system with increased refractive indices of the second and third layer is investigated. We employ a wavelength-independent refractive index for all three layers, with refractive indices of the layers I, II and III set to 1.5, 2.5 and $3.5 + 0.5i$. Also for this system the wavelength

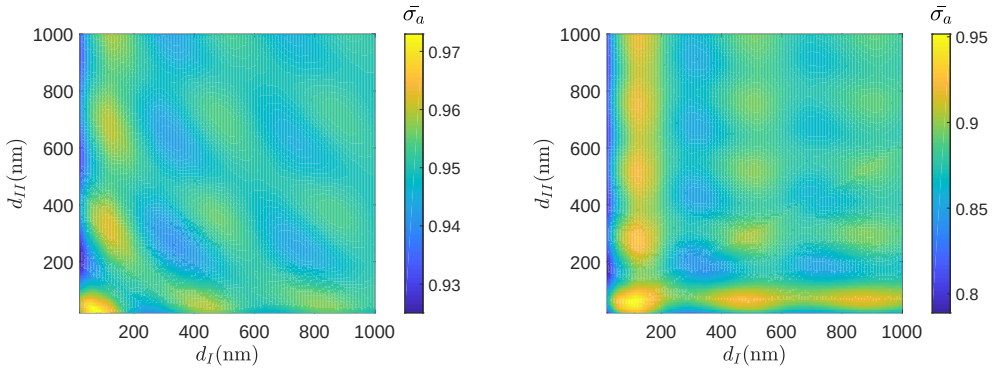


(a) (b)

Figure 6: The average absorption cross section, $\bar{\sigma_a}$, for a three layer system as in Fig. 1b is shown as a heat map for varying thicknesses of the two first non-absorbing layers. The thickness of the two first layers are varied between 20 nm and 1000 nm. The thickness of the third layer is kept constant at 1000 nm. The refractive indices of the layers are (a) $n_I = 1.5$, $n_{II} = 1.65$, and $n_{III} = 1.8+0.3i$ and (b) $n_I = 1.5$, $n_{II} = 2.5$, and $n_{III} = 3.5+0.3i$, respectively. The wavelength range that is investigated is 200 nm - 1200 nm.

range evaluated is 200-1200 nm. The thicknesses of the two first layers are changed between 20 nm and 1000 nm and the thickness of the third layer is 1000 nm.

A comparison between Fig. 6a and Fig. 6b shows that the benefits of choosing the correct thickness of the first two layers are higher for systems where the differences of refractive indices of the layers are larger. For a system as described in Fig. 6b, an optimization of the thicknesses could give more than 15 % increase of the the average absorption cross section.

## 3. OPTIMIZATION OF ABSORPTION OF THIN-FILM SOLAR CELLS

In this section we will show how considering resonances in thin-film systems can help to optimize experimentally realizable solar cells. We consider the system shown in Fig 7b, which is a simplification of a five-layer epitaxial crystalline silicon solar cell, which is optically thin as shown in Fig. 7a.[19] The experimentally realized system consists of three different materials, ITO, amorphous silicon and crystalline silicon, the two silicon layers consists of p-doped and one n-doped layers as shown in the figure. In order to simplify the system, we treat the amorphous silicon as one layer with the same wavelength dependent refractive index. The same assumption is used for the crystalline silicon. The absorption cross section is calculated by Eq. 1, and the refractive index of the three layers that are used are experimentally determined.[20–22] By evaluating the absorption cross section for different choices of thickness for the three layers, the system can be optimized to absorb as much radiation as possible.

The system in Fig. 7b is evaluated for several thicknesses of the layers. The average absorption cross section, $\bar{\sigma_a}$ is shown for systems with c-Si film thickness equal to 0.5 µm, 2 µm, 8 µm, 32 µm, 100 µm and 200 µm in Fig. 8. The thicknesses of the two first layers are varied between 20 nm and 500 nm. We investigated the wavelength range from 250 nm to 1000 nm. Since the photon energy exceeds the 1.1 eV band gap of silicon,[23] radiation in the investigated spectral range is absorbed. As Fig. 8 indicates, certain combinations of thicknesses of the two first layers give higher $\bar{\sigma_a}$ values than other.

As Fig. 8 indicates, 60 nm and 150 nm are optimal thicknesses for the first and the second layer, respectively. We therefore set the thicknesses of the first and second layers to 60 nm and 150 nm, and vary now the thickness of the third layer. By continuously increasing the thickness of the third layer from 0.5 µm to 200 µm, the findings of Sec. 2.1.2 are confirmed: When the thickness of the energy converting layer is increased, the average absorption cross section $\bar{\sigma_a}$ stabilizes at a certain value. This is shown in Fig. 9, where the average absorption cross section $\bar{\sigma_a}$ is shown as a function of the thickness of the third layer. We observe that the $\bar{\sigma_a}$ stabilizes at a maximum value of approximately $\bar{\sigma_a} = 0.8$. The stabilization takes place at when the thickness of the third layer is approximately 50 µm. For larger thicknesses no further enhancement of the absorption of the c-Si layer

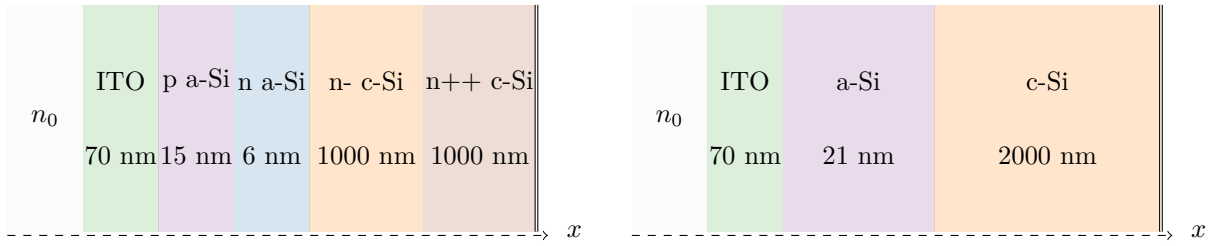


(a) (b)

Figure 7: A multilayer thin-film solar cell consisting of five thin layers and a mirror are shown in (a). This solar cell has been experimentally realized[19] and consists of ITO, n- and p-doped amorphous and crystalline silicon. The thickness of the layers of the experimentally realized system is shown in the model. The system has been simplified into a three-layered system with mirror (b).[8] The system has been simplified by replacing the layers with different doping with one single layer with experimentally determined refractive index.[20–22] $n_0$ indicates the refractive index of vacuum, $n_0 = 1$. Behind the layers of the different material a perfect mirror is placed. In order to optimize the system, the thicknesses of the three layers are changed.The result of this is shown in Fig. 8.

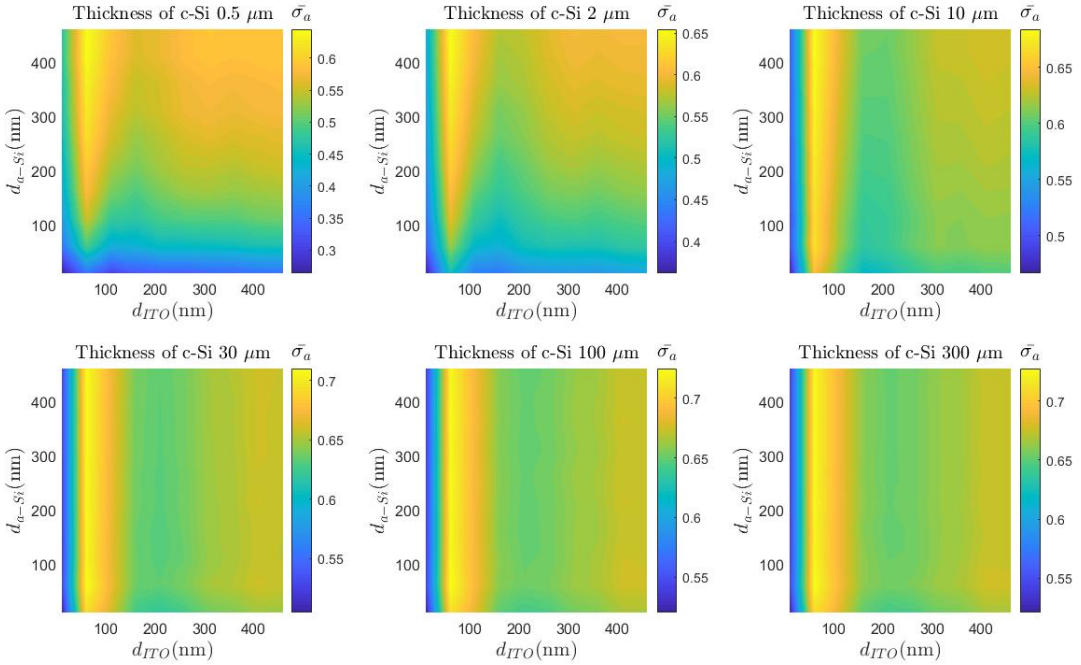


Figure 8: The average absorption cross section, $\bar{\sigma_a}$, for a three film system with the same materials as shown in Fig. 7b with experimentally determined refractive indices.[20–22] The thickness of the two first layers are varied between 20 nm and 500 nm. The thickness of the c-Si layer is set to 0.5 µm, 2 µm, 8 µm, 32 µm, 100 µm and 200 µm respectively. The wavelength range that is investigated is from 250 nm to 1000 nm.

can be obtained. A further investigation of the material cost versus the absorption efficiency is needed in order to decide if a thickness of 50 µm is an optimum, since already a thickness of the c-Si layer of around 20 µm is close to the optimum value for the average absorption cross section $\bar{\sigma_a}$ .

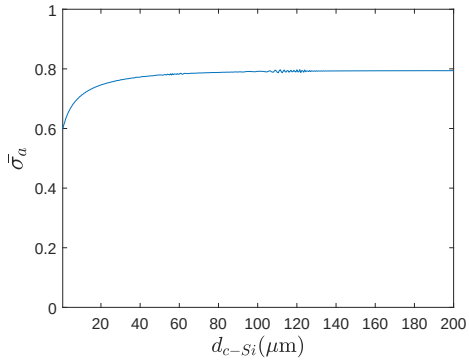


Figure 9: The average absorption cross section, $\bar{\sigma_a}$, as function of the thickness of the c-Si layer. The system is equivalent to the system shown in Fig. 7b where the thicknesses of ITO and a-Si are set to 60 nm and 150 nm, respectively. Further, the thickness of the c-Si layer, $d_{c-Si}$, is increased from 0.5 µm to 200 µm. The refractive indices of the layers are experimentally determined.[20–22]

## 4. DISCUSSION

The results presented in Sec. 2 show that when the imaginary part of the refractive index of the absorptive material is changed, the resonant structure of the absorption cross section and the absorption properties of the material change. When the imaginary part of the refractive index of the absorptive material increases, the electromagnetic field in the film system goes from a resonance structure formed by standing waves that are extended over both films to a resonance structure that consists of resonances only in the first film. For large imaginary part of the refractive index, all radiation entering the absorptive material is absorbed before it reaches the mirror. Therefore, standing wave do not occur the absorptive material for large imaginary part of the refractive index. One might assume an increasing imaginary part of the refractive index results in an increased absorption cross section. However, as confirmed by the Fresnel equations,[11] the reflection from the absorbing film's surface increases when the imaginary part of the refractive index increases. Therefore, less radiation is transmitted into the absorptive material, which results in lower absorption. As Figs. 2 and 3 show, there is an optimal size of the imaginary part of the refractive index of the absorptive material, where the wave function is just totally absorbed before it reaches the mirror. Since we consider the average absorption cross section for a whole wavelength region, this condition of optimal imaginary part of the refractive index is achieved, when the standing wave in the absorbing material is just disappeared for small wavelengths, while it is present for large wavelengths. When investigating the absorption properties of the film system as a function of the thickness of the absorbing film, we observe that the absorption increases with increasing thickness of the absorbing layer until a maximum is reached and stays constant for larger thicknesses. In general we see that absorption in the absorbing layer is enhanced by resonances in the non-absorptive material, which lead to an field enhancement in the absorbing material.

When considering a system consisting of three layers, we find that it is important to investigate first all combinations of thicknesses of the first two layers in order to optimize the thicknesses of the first two layers. The optimal thickness of the third layer is then found, where the wave function is just totally adsorbed. Further we find that the benefits of the optimization is larger for systems with larger differences in refractive indexes in the different films

In section 3, the absorption cross section for experimentally realizable thin-film solar cells are investigated. A experimentally realized solar cell was used as a template, and experimentally determined refractive indices were used in the system. The observations were comparable to the results found in Sec. 2 where systems with wavelength independent refractive indices are investigated.

In all systems considered, we were studying the average absorption cross section, $\bar{\sigma_a}$. It is important to notice that $\bar{\sigma_a}$ changes if we change the wavelength range. It is therefore essential to optimize the system according to the proper wavelength range. In our study, the results presented were not weighted with the solar spectrum. If the absorption cross section is weighted with the solar spectrum, the optical generation rate[10] is obtained. In order to further evaluate a thin-film solar cell system, the average optical generation rate should be evaluated.

Our model is exact for situations with coherent light, which is a common assumption for simulations of thin-film solar cells where the thickness of the films is smaller then the coherence wavelength.[24] Sunlight, however, is incoherent, so the assumption of coherent light in our model is not strictly applicable to the case of incoherent sunlight. Indeed, it is known that there is a difference in conversion efficiency between illumination with coherent and incoherent light.[25] Since the spatial coherence area of sunlight is about 60 µm × 60 µm,[26] and resonant solar-cell surface structures are of the order of a micron, the effects of spatial coherence may be neglected. However, since the temporal coherence length of sunlight is about 600 nm,[27] and the thicknesses of our films are about of this order of magnitude, the temporal incoherence of sunlight cannot be neglected. Therefore, while our results are rigorous for coherent incident light, we have to be careful when using these results to make predictions for the case of incoherent sunlight. On the upside, a two-step method exists that takes the results of coherent calculations as input for a folding step that then obtains conversion efficiencies for incoherent illumination directly from the coherent input.[25,28] Therefore, our results presented here are the first step in this two-step process. We hope that after conversion to incoherent light our predictions still hold. We have not yet performed this second step, but plan to investigate it next.

For monochromatic light, our results indicates that the optimum in conversion efficiency is reached when the layers in front of the energy-converting material are around the same size as the coherence length of the light.[27] We could therefore expect resonances in the first layers. Further, we show that it is optimal that the energy converting material should have a thickness so that the wave function is totally absorbed before it reaches the mirror. In this cases we will not have resonances in the layer closest to the mirror. We hope that these predictions, based on a coherent, monochromatic model are robust and will also hold in the case of illumination with incoherent light.

Our model only evaluates the optical properties of the system. Effects linked to losses other than reflection are not included in our models.

## 5. CONCLUSION

In this paper we have shown that simple calculations of the absorption cross section can give an indication of a proper choice of thickness of the layers in a thin-film solar cell. We find that a resonance in the front layers can result in an increased absorption cross section. This is caused by the enhanced wave function in the front layers. Due to the continuity of the wave function this also results in an enhanced absorption of radiation in the absorptive material. We have also shown that the absorption cross section decreases when the imaginary part of the refractive index of the absorptive material increases. This is because the reflection probability increases according to Fresnel's equations. An optimal imaginary part of the refractive index is therefore obtained when the absorption is high enough such that standing waves just disappear in the absorbing material for a large part of the wavelength region considered, but not too high such that not a too large part of the radiation is reflected in the energy converting material. We have applied our findings wit success to the optimization of an experimentally realizable solar cell system.

## ACKNOWLEDGMENTS

This work was supported by the grant *Development of a new ray model for understanding the coupling between dielectric spheres for photovoltaics with higher efficiency*, No: 250678. Financed by The Research Council of Norway.

## REFERENCES


[1] Brendel, R., [*Thin-film crystalline silicon solar cells: physics and technology*], John Wiley & Sons (2011).

[2] Lee, T. D. and Ebong, A. U., "A review of thin film solar cell technologies and challenges," *Renewable and Sustainable Energy Reviews* **70**, 1286–1297 (2017).

[3] Grandidier, J., Callahan, D. M., Munday, J. N., and Atwater, H. A., "Light absorption enhancement in thin-film solar cells using whispering gallery modes in dielectric nanospheres," *Advanced Materials* **23**(10), 1272–1276 (2011).

[4] Kang, G., Park, H., Shin, D., Baek, S., Choi, M., Yu, D. H., Kim, K., and Padilla, W. J., "Broadband light-trapping enhancement in an ultrathin film a-si absorber using whispering gallery modes and guided wave modes with dielectric surface-textured structures," *Adv Mater* **25**(18), 2617–23 (2013).

[5] Becker, C., Wyss, P., Eisenhauer, D., Probst, J., Preidel, V., Hammerschmidt, M., and Burger, S., "5x5 cm2 silicon photonic crystal slabs on glass and plastic foil exhibiting broadband absorption and high-intensity near-fields," *Scientific Reports* **4**, 5886 (2014).

[6] ElAnzeery, H., El Daif, O., Buffière, M., Oueslati, S., Ben Messaoud, K., Agten, D., Brammertz, G., Guindi, R., Kniknie, B., Meuris, M., and Poortmans, J., "Refractive index extraction and thickness optimization of cu2znsnse4 thin film solar cells," *physica status solidi (a)* **212**(9), 1984–1990 (2015).

[7] Saylan, S., Milakovich, T., Hadi, S. A., Nayfeh, A., Fitzgerald, E. A., and Dahlem, M. S., "Multilayer antireflection coating design for gaas0.69p0.31/si dual-junction solar cells," *Solar Energy* **122**, 76 – 86 (2015).

[8] Brandsrud, M., Seim, E., Lukacs, R., Kohler, A., Marstein, E., Olsen, E., and Blümel, R., "Exact ray theory for the calculation of the optical generation rate in optically thin solar cells," *Physica E: Low-dimensional Systems and Nanostructures* **105**, 125–138 (2019).

[9] Hulst, H. C. and van de Hulst, H. C., [*Light scattering by small particles*], Courier Corporation (1981).

[10] Ferry, V. E., Munday, J. N., and Atwater, H. A., "Design considerations for plasmonic photovoltaics," *Adv Mater* **22**(43), 4794–808 (2010).

[11] Sadiku, M. N., [*Elements of electromagnetics*], Oxford university press (2014).

[12] Townsend, J., [*Quantum Physics: A Fundamental Approach to Modern Physics*], University Science Books (2010).

[13] Griffiths, D. J., [*Introduction to electrodynamics*], Prentice Hall, Upper Saddle River, N.J, 3rd ed. ed. (1999).

[14] Cozza, D., Ruiz, C. M., Duché, D., Giraldo, S., Saucedo, E., Simon, J. J., and Escoubas, L., "Optical modeling and optimizations of cu 2 znsnse 4 solar cells using the modified transfer matrix method," *Optics express* **24**(18), A1201–A1209 (2016).

[15] Schmid, M., "Review on light management by nanostructures in chalcopyrite solar cells," *Semiconductor Science and Technology* **32**(4), 043003 (2017).

[16] Uematsu, T., Ida, M., Hane, K., Hayashi, Y., and Saitoh, T., "New light trapping structure for very-thin, high-efficiency silicon solar cells," *Conference Record of the IEEE Photovoltaic Specialists Conference* **1**, 792–795 (1988). cited By 5.

[17] Yablonovitch, E., "Statistical ray optics," *J. Opt. Soc. Am.* **72**, 899–907 (Jul 1982).

[18] Campbell, P. and Green, M. A., "Light trapping properties of pyramidally textured surfaces," *Journal of Applied Physics* **62**(1), 243–249 (1987).

[19] Selj, J. K., Young, D., and Grover, S., "Optimization of the antireflection coating of thin epitaxial crystalline silicon solar cells," *Energy Procedia* **77**, 248–252 (2015).

[20] Green, M. A., "Self-consistent optical parameters of intrinsic silicon at 300 k including temperature coefficients," *Solar Energy Materials and Solar Cells* **92**(11), 1305–1310 (2008).

[21] Pierce, D. and Spicer, W. E., "Electronic structure of amorphous si from photoemission and optical studies," *Physical Review B* **5**(8), 3017 (1972).

[22] König, T. A., Ledin, P. A., Kerszulis, J., Mahmoud, M. A., El-Sayed, M. A., Reynolds, J. R., and Tsukruk, V. V., "Electrically tunable plasmonic behavior of nanocube–polymer nanomaterials induced by a redox-active electrochromic polymer," *ACS nano* **8**(6), 6182–6192 (2014).

[23] Shimadzu, "Band gap measurement of polycrystalline silicon wafer," (2014).

[24] Puhan, J., Lipovšek, B., Bűrmen, A., and Fajfar, I., "An accurate representation of incoherent layers within one-dimensional thin-film multilayer structures with equivalent propagation matrices," *IEEE Photonics Journal* **9**, 1–12 (Oct 2017).

[25] Herman, A., Sarrazin, M., and Deparis, O., "The fundamental problem of treating light incoherence in photovoltaics and its practical consequences," *New Journal of Physics* **16**(1), 013022 (2014).

[26] Agarwal, G. S., Gbur, G., and Wolf, E., "Coherence properties of sunlight," *Optics letters* **29**(5), 459–461 (2004).

[27] Donges, A., "The coherence length of black-body radiation," *European journal of physics* **19**(3), 245 (1998).

[28] Sarrazin, M., Herman, A., and Deparis, O., "First-principle calculation of solar cell efficiency under incoherent illumination," *Optics express* **21**(104), A616–A630 (2013).